An Enhanced Ivy Algorithm for Maximum-Power-Point Tracking in Photovoltaic Systems

Yuhang Kang, Lidong Wang*, Zhongfeng Li*, Mingyang Liu, Zhenlong Zhao, and Lei Liu

Abstract—Accurate maximum-power-point tracking (MPPT) is crucial for photovoltaic (PV) systems under rapid variations in irradiance and temperature. This study proposes an improved Ivy algorithm (IIVY) incorporating reverse-learning population initialization, an adaptive growth factor, and Lévy-flight updates to enhance diversity, accelerate convergence, and avoid local optima. Evaluated on the CEC-2017, CEC2020 and CEC2022 benchmark, IIVY achieves top-ranking mean performance across 29 functions in both 50- and 100-dimensional scenarios. Embedded into a MATLAB/Simulink-based single-diode PV MPPT controller under step irradiance transitions (1000 \rightarrow $700 \rightarrow 400 \,\mathrm{W\,m^{-2}}$), IIVY increases harvested energy by 6.53%, 4.59%, 7.73%, and 13.26% compared to IVY, PSO, BAT, and GA, respectively. It also reduces settling times to 0.15-0.25 s and power fluctuations by up to 78%. These findings highlight IIVY as an efficient and robust real-time MPPT solution for advanced PV converters.

Index Terms—Ivy Algorithm, Photovoltaic Arrays, Maximum-Power-Point Tracking, Meta-heuristic Optimisation.

I. Introduction

W ITH the continuous growth of global energy demand and the increasing depletion of fossil energy sources, the proportion of renewable energy in the energy structure has been increasing, further accelerating the transition to clean energy. Currently, renewable energy has accounted for

Manuscript received July 8, 2025; revised September 21, 2025.

This work was supported in part by the Fundamental Research Funds for Liaoning Provincial Joint Funds Project - General Funding Program (Grant Nos. 2023-MSLH-323 and 2023-MSLH-310); the Fundamental Research Funds for Liaoning Universities (Grant No. LJ212410146009); 2025 scientific research fund project of Liaoning Provincial Department of Education (Grant No. LJ212514435004 and Grant No. LJ212514435006); 2022 scientific research fund project of Liaoning Provincial Department of Education (Grant No. LJKFZ20220292 and Grant No. LJKMZ20221859); the Foundation of Yingkou Automation Industrial Control Professional Technology Innovation Center (Grant No. AICPTI02); the Foundation of Yingkou Institute of Technology under the Institutional-Level Scientific Research Initiative (Grant Nos. FDL202404 and FDL202409).

Yuhang Kang is a postgraduate of School of Electronic and Information Engineering, University of Science and Technology Liaoning, Anshan 114051 China (e-mail:18524333009@163.com).

Lidong Wang is a professor at the School of Electronic and Information Engineering, University of Science and Technology Liaoning, Anshan 114051 China (corresponding author, e-mail: wangld5600@163.com).

Zhongfeng Li is an associate professor of School of Electrical Engineering, Yingkou Institute of Technology, Yingkou, 115100 China (corresponding author, e-mail: afeng0601@163.com).

Mingyang Liu is a postgraduate of School of Electronic and Information Engineering, University of Science and Technology Liaoning, Anshan 114051 China (e-mail:w1094552272@163.com).

Zhenlong Zhao is an associate professor of School of Electrical Engineering, Yingkou Institute of Technology, Yingkou, 115100 China(e-mail: zhaozhenlong@yku.edu.cn).

Lei Liu is an associate professor at the School of Mechanical Engineering, Yingkou Institute of Technology, Yingkou, 115100 China(e-mail: liulei@yku.edu.cn).

26.3% of the global energy mix, with hydropower accounting for 15.8%, wind energy for 5.3%, solar energy for 2.7%, and the remaining renewable energy sources accounting for 2.5% [1]. By diversifying the energy structure, solar, wind, and biomass not only effectively reduce greenhouse gas emissions, but also significantly improve energy security. Among them, solar PV power generation has attracted much attention due to its cleanliness, sustainability, and decreasing cost. The structure of PV systems is relatively simple and economically sound, and as of 2019, the cumulative global installed PV capacity has reached 627 GW, with a new installed capacity of 115 GW in that year [2]. However, the output power of PV arrays is significantly affected by light intensity and ambient temperature, and in order to fully utilize PV resources under different operating conditions, MPPT technology has become the key to improving system power generation efficiency [3]. Since the maximum power point changes with external conditions, and the PV I-V curve may have multiple peaks under complex operating conditions such as partial shading, the MPPT algorithm needs to have a strong global optimization capability.

Conventional MPPT methods, such as the perturbation observation (P&O) [4] and incremental conductance (IC) [5] methods, although variously improved and fused, usually only show a high level of efficiency under conditions of uniform and slowly varying irradiance distribution and show high efficiency. Under complex conditions such as partial shading, multi-directional light changes, or sudden temperature changes, such methods are prone to fall into local optimization, thus missing the global MPPT [6]. To solve the optimization problem under multi-peak I-V curves, intelligent optimization algorithms based on the principle of meta-heuristics have been gradually introduced into PV MPPT control, such as Genetic Algorithms (GA), Particle Swarm Optimization (PSO), and Bat Algorithms (BAT) [7]. These algorithms achieve large-scale exploration of the solution space by simulating population behavior or natural evolutionary mechanisms, and possess strong global search capability with the ability to jump out of the local optimum, and thus can achieve excellent performance in highly nonlinear and nonconvex PV system optimization problems. However, these intelligent algorithms usually require a large amount of computational resources during the iterative process, resulting in relatively slow convergence, especially in real-time embedded photovoltaic control systems, where computational delays can directly affect the energy capture efficiency [8]. In response to rapidly changing meteorological conditions, current studies generally agree that a balance should be struck between tracking accuracy and computational speed [9]. One feasible way is to combine intelligent optimization algorithms with classical MPPT methods, using the fast response advantage of the latter complemented by the global optimization capability of the former, so as to achieve a more stable performance under dynamic working conditions [10, 11]. In addition, the digital twin technology that has emerged in recent years offers new possibilities for monitoring and optimization of PV systems [12]. By constructing a virtual model that is highly consistent with the physical system, digital twins can not only realize real-time state mirroring but also combine with predictive control strategies to adjust the MPPT operating parameters in advance, thus enhancing the system's adaptive capability and reducing hardware dependence [13].

With the continuous development of technology and the growing demand for higher energy conversion efficiency [14], the combination of intelligent optimization algorithms and MPPT technology has become an important way to improve the performance of PV systems [15]. It has been shown that meta-heuristics such as GA [16] and PSO [17] are excellent in global optimization and tracking performance in variable environments, but their high computational overheads and slow convergence speeds limit their application in real-time PV control. To overcome these limitations, the Ivy optimization algorithm (IVY) [18], proposed in recent years, shows potential for application in MPPT by virtue of its simple mathematical structure and strong global search capability. However, under high-dimensional optimization and complex dynamic conditions, IVY is prone to problems such as premature convergence and falling into a local optimum, which affects the accurate location of the global MPPT [19] under the rapidly changing conditions of light and temperature. To address the above deficiencies, this study proposes an improved IVY algorithm, which dynamically adjusts the algorithm parameters according to environmental changes by introducing an adaptive mechanism to enhance global search capability and improve tracking accuracy. In addition, the algorithm also combines a hybrid meta-heuristic strategy with a real-time adaptive control method to further enhance the robustness and stability, which results in a better performance in dealing with the PV MPPT problem with high-dimensional, nonlinear, and multi-peak characteristics. The improved IVY, when integrated with the MPPT control strategy, not only achieves faster convergence speed and higher localization accuracy but also effectively improves the solar energy conversion efficiency under transient and steady state conditions, providing an efficient and reliable control scheme for the next generation of high-performance PV systems.

The main contributions of this study are:

- (1) Development of IIVY, an enhanced IVY integrating reverse-learning initialization, adaptive growth factors, and Lévy-flight updates to significantly boost search efficacy and convergence performance.
- (2) Validation of IIVY through extensive comparisons against eight benchmark algorithms using CEC-2017 functions. Experimental outcomes and statistical analyses confirm superior performance across diverse optimization scenarios.
 - (3) Successful deployment of IIVY in MPPT tasks,

demonstrating substantial improvements over traditional algorithms (PSO, GA, BAT, IVY). Results illustrate enhanced tracking precision, faster convergence, and reduced power fluctuations under dynamic irradiance conditions.

The remainder of this paper is organized as follows. Section II outlines the fundamental principles of the original IVY algorithm. Section III presents the proposed IIVY algorithm, including its novel initialization, update strategies, and adaptive mechanisms. Section IV reports the results of benchmark experiments on the CEC 2017, CEC 2020, and CEC 2022 test suites, followed by statistical analyses and comparisons with other meta-heuristic algorithms. Section V demonstrates the application of IIVY to MPPT in photovoltaic systems under dynamic irradiance conditions. Finally, Section VI concludes the study and discusses possible directions for future research.

II. BASIC PRINCIPLE OF THE IVY

The IVY algorithm proposed by Mujtaba Gha et al. (2024) models the adaptive and biologically inspired growth strategy of natural climbing plants: first gradually spreading widely and horizontally across the ground surface, then rapidly ascending upward toward sunlight once reliable structural support is eventually found, thereby significantly accelerating overall development. The algorithm carefully quantifies growth rates through mathematical differential equations and also incorporates relevant experimental data. It further realistically simulates cooperative path optimization among individual plants based on spatial proximity and ecologically categorizes diverse climbers according to complex real-time environmental conditions.

- Plants that thrive indoors but perform poorly outdoors.
- Climbing plants well adapted to natural outdoor environments.

A. IVY Mathematical Model

The IVY algorithm mimics the main phases of ivy growth: initial expansion, vertical ascent, and continuous spread. Conceptually, IVY can be divided into three stages:

Step 1: Direct population growth in an orderly fashion.

Step 2: Grow toward the light source.

Step 3: Continuously spread and evolve.

At the start, a cluster of ivy trees represents candidate solutions to the optimization task. Each tree's location in the search space is defined by its position vector, and its growth rate is computed. Individuals are ranked by fitness from best to worst.

Positions are iteratively adjusted based on fitness values (the objective function). As individuals move toward the light source, the collective population converges toward the global optimum. The mathematical model of IVY is detailed below.

Initialization: N_{pop} and D denote the population size and number of decision variables, respectively. For the ivy population, we define $\overrightarrow{I} = (I_1, \dots, I_i, \dots, I_{N_{\text{pop}}})$, where $i = 1, 2, \dots, N_{\text{pop}}$. Initial positions are generated as:

$$I_i = I_{\min} + \operatorname{rand}(1, D) \cdot (I_{\max} - I_{\min}) \tag{1}$$

where i denotes the i-th individual, rand is uniformly distributed over [0,1], and I_{\min} , I_{\max} are the lower and upper bounds.

Search and exploration: The IVY growth process is described in three steps.

Step 1: Orderly population growth. IVY expands by following sunlight. Its growth rate G_v is modeled as:

$$\frac{dG_v(t)}{dt} = \psi \cdot G_v(t) \cdot \varphi(G_v(t)) \tag{2}$$

where G_v is the growth rate, and ψ , φ represent parameters capturing deviations in rate and direction. The discrete-time update is:

$$\Delta G_{v_i}(t+1) = \operatorname{rand}^2 \cdot (N(1,D) \cdot \Delta G_v(t)) \tag{3}$$

where rand is uniformly sampled from [0,1], rand² denotes a random variable with PDF $1/(2\sqrt{x})$, and N(1,D) is a D-dimensional vector with standard normal components.

Step 2: Growth toward light. Inspired by ivy climbing supports (e.g., walls or trees) to reach light, the algorithm simulates competition and improvement by referencing nearby neighbors selected by fitness. For the sorted population $T_s = [I^1, \ldots, I^s]$, with $I_{\text{best}} = I^1$:

$$I_{ii} = \begin{cases} I_{j-1}^{s}, & I_{i} = I_{j}^{s}, \\ I_{i}, & I_{i} = I_{\text{best}}. \end{cases}$$
(4)

Movement toward light is given by:

$$I_i^{\text{new}} = I_i + |N(1, D)| \cdot (I_{ii} - I_i) + N(1, D) \cdot \Delta G_{v_i} \quad (5)$$

$$\Delta G_{v_i} = \begin{cases} I_i / (I_{\text{max}} - I_{\text{min}}), & \text{Iter} = 1, \\ \\ \text{rand}^2 \cdot (N(1, D) \cdot \Delta G_{v_i}), & \text{Iter} > 1. \end{cases}$$
 (6)

where |N(1,D)| denotes the elementwise absolute value of the normal vector.

Step 3: Spread and evolution. Once I_i moves toward its nearest neighbor I_{ii} , it proceeds to refinement. Here, I_i follows I_{best} , expressed as:

$$I_i^{\text{new}} = I_{\text{best}} + (\text{rand}(1, D) + N(1, D)) \cdot \Delta G_{v_i}$$
 (7)

The updated growth rate is:

$$\Delta G_{v_i}^{\text{new}} = I_i^{\text{new}} \cdot (I_{\text{max}} - I_{\text{min}}) \tag{8}$$

Survivor selection: Horlacher and Bauer [18] examined stage-dependent light requirements. In early stages, stronger absorption is needed; later, less. The algorithm mimics "upward climbing" and "lateral expansion": if an individual's fitness is below a threshold proportional to $f(I_{\rm best})$ (controlled by $\beta=\frac{2+{\rm rand}}{2}$), it expands laterally (Eq. 5); otherwise, it climbs upward (Eq. 7). At each iteration, previous individuals I and new candidates $\vec{I}^{\rm new}$ are combined and ranked by fitness to form $\vec{I}^{M/S}$. The best $N_{\rm pop}$ individuals are retained for the next generation.

III. THE PROPOSED IIVY

The basic IVY shows superior performance on complex optimization problems but faces practical limitations due to inefficient search, difficulty reconciling convergence speed and accuracy, and a tendency to fall into local optima (premature convergence) caused by loss of population diversity in multi-peak function optimization. To address these shortcomings, three enhancements have been developed.

A. Create a New Initialization Population Formula

The random initial population of traditional IVY is prone to uneven distribution and poor diversity in high-dimensional complex problems, leading to weak global search and premature convergence. To overcome this, we integrate the inverse learning principle to optimize population generation. By generating symmetric solution points, this strategy significantly improves the diversity and quality of the initial population, ensures wider search coverage, and effectively avoids local optima, thus laying a highly efficient foundation for subsequent optimization. This ultimately achieves significant improvements in convergence speed and solution accuracy, as shown in Eq. (9):

$$I_i^{\text{opp}} = I_{\min} + \text{rand}(1, D) \cdot (I_{\max} - I_{\min}) - I_i \tag{9}$$

where D is the problem dimension, and I_{\min} and I_{\max} are the lower and upper bound vectors of each dimension. A random matrix with the same population size and problem dimensions introduces randomness in generating inverse solutions. The initial and inverse populations are combined, fitness is calculated for each individual, and the top N individuals with higher fitness are selected as the final initial population.

B. New Position Update Formula

The IVY algorithm is prone to local optimization and lacks an effective escape mechanism, leading to weak global search, slow convergence, and difficulty improving accuracy in later stages. To overcome these limitations, this paper introduces a position update strategy based on Lévy flights. The heavy-tailed distribution characteristic of Lévy flights allows for long-distance jumps during the search, enhancing the algorithm's global exploration capability and increasing the probability of escaping local optima. Simultaneously, this strategy maintains population diversity, preventing premature convergence. By promoting a balanced exploration of the solution space, the algorithm avoids excessive focus on local regions, thereby improving optimization search performance. As shown in Eqs. (11) and (12), the Lévy flight update rule dynamically adjusts the search path, enabling efficient exploration of the solution space, ultimately improving overall optimization performance.

$$L = \frac{0.01 \cdot u}{|v|^{\beta}} \tag{10}$$

where L is the Lévy step generated according to the properties of the Lévy distribution. u is a random variable following a normal distribution, $u \sim N(0,\sigma^2)$; v is also normally distributed, $v \sim N(0,1)$; β is a parameter of the Lévy distribution, usually $\beta \in (1,2)$, controlling step-size characteristics. The factor 0.01 is a scaling factor to adjust the step size for specific problems. The updating method introduces an adaptive convergence factor that can dynamically adjust the growth vector according to:

$$I_i^{\text{new}} = I_i + |N(1, D)| \cdot (I_{ii} - I_i) + N(1, D) \cdot \Delta G_{v_i} + L,$$
if $f(I_i) < f(I_{\text{best}})$
(11)

$$I_i^{\text{new}} = I_{\text{best}} \cdot (\text{rand}(1, D) + N(1, D)) \cdot \Delta G_{v_i},$$

$$\text{if } f(I_i) > f(I_{\text{best}})$$

$$(12)$$

C. New Formula for Updating G_v

The standard IVY uses a fixed update rule for the growth rate, which cannot adapt to the requirements of different optimization stages. In the early phase, its global search ability is limited, and initialization often fails to achieve full exploration. In later stages, the algorithm is prone to stagnation in local optima, preventing discovery of the best solution. These shortcomings reduce efficiency and contribute to premature convergence. To address this, an adaptive convergence factor is introduced that adjusts the step size dynamically according to the stage of the search. At the beginning, a larger step size supports wide global exploration and increases diversity. As iterations progress, the step size gradually decreases, enabling fine local refinement, improving accuracy, and reducing the risk of falling into local traps. This adaptive adjustment both accelerates convergence and prevents premature stagnation. The formulation is given in Eq. (14), where the factor changes at each iteration to balance exploration and exploitation.

$$w = 1.5 - \frac{1}{1 + k_1 \cdot \exp(-k_2 \cdot t)},\tag{14}$$

where $k_1=1$ and $k_2=0.1$ are adjustable parameters that control the variation of the convergence factor, and t is the current iteration index.

$$\Delta G_{v_i}^{\text{new}} = \text{rand}^2 \cdot (N(1, D) \cdot \Delta G_{v_i}) \cdot w \tag{13}$$

The overall procedure is illustrated in Fig. 1.

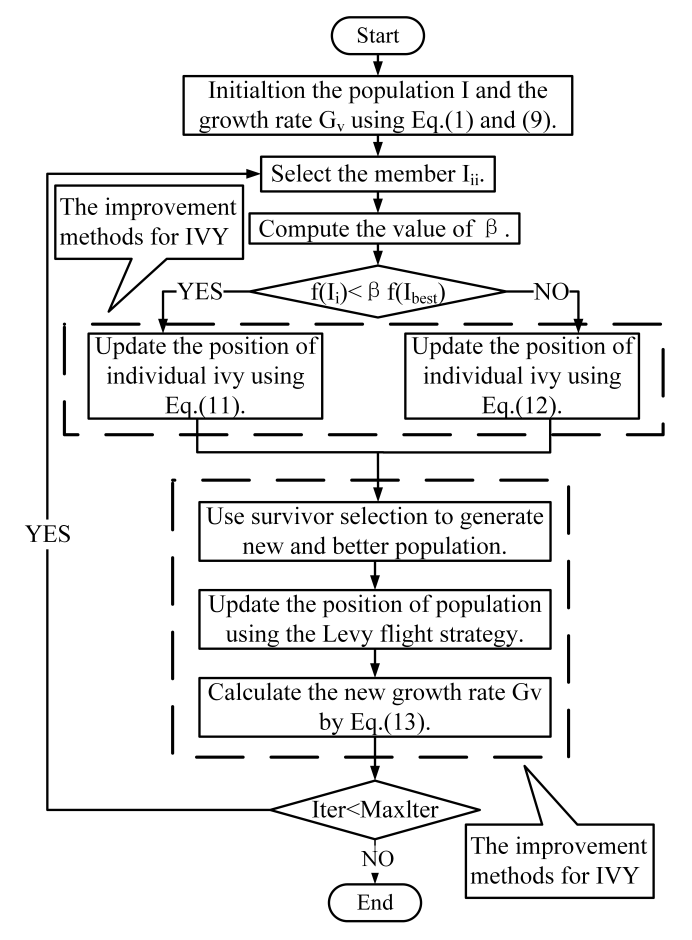


Fig. 1: The flowchart of IIVY.

IV. RESULTS OF EXPERIMENT AND STATISTICAL ANALYSIS

A. Benchmark Functions

To comprehensively evaluate algorithm performance, three authoritative benchmark test suites are adopted: CEC 2017 [19], CEC 2020 [20], and CEC 2022 [21]. These cover problems of varying complexity and characteristics, allowing a thorough assessment in terms of convergence speed, ability to escape local optima, adaptability to complex landscapes, and effectiveness in global search.

The CEC 2017 set includes four categories: F1-F3 test convergence speed, F4-F10 evaluate the ability to escape local optima, F11-F20 examine adaptability to complex landscapes, and F21-F30 assess performance on composite functions. CEC 2020 is divided into four types as well: single-peak (F1), multi-peak (F2-F4), hybrid (F5-F7), and combinatorial (F8-F10), designed to evaluate convergence speed, robustness against multi-peak local traps, and adaptability to hybrid and combinatorial problems. CEC 2022 also contains four categories: single-peak (F1), multi-peak (F2-F5), hybrid (F6-F8), and combined (F9-F12). These functions emphasize algorithm stability in dynamic environments, global search efficiency, and adaptability to dynamic or composite problems. The multidimensional classification provided by these test suites enables a systematic evaluation of generalization capability and robustness under diverse conditions of problem scale, complexity, and dynamics.

B. Comparison with Other Algorithms

Using the above benchmark sets, a comprehensive comparison is conducted between the improved IVY (IIVY), the basic IVY, and eight other widely used optimization algorithms. To ensure fairness, all algorithms are run with standardized parameter settings, which are detailed in Table I. The experiments are performed in 20-, 50-, and 100-dimensional spaces, thereby increasing the level of challenge and providing a closer approximation to real-world complex optimization scenarios.

The evaluation metrics include mean, standard deviation, best value, and rank. These important and widely used indicators together offer a more complete and comprehensive picture of performance across different functions, thoroughly covering convergence rate, accuracy, stability, and robustness. Results are clearly summarized in Tables III and VIII. For more detailed and in-depth analysis, one or two carefully chosen representative functions are selected from each category in the three benchmark sets, mainly focusing on convergence behavior and noticeable changes in population diversity. These detailed outcomes are finally presented in Tables IV, V, VI, and VII.

The convergence curves and diversity dynamics, shown in Fig. 2 and Fig. 3, provide an intuitive, and comprehensive demonstration of algorithm behavior during the entire iterative optimization process. The detailed experimental findings strongly indicate that IIVY consistently and reliably escapes undesirable local optima much more effectively than the baseline IVY while still successfully maintaining higher population diversity, thereby effectively avoiding premature convergence and steadily achieving significantly higher overall optimization efficiency.

TABLE I PARAMETER SETTINGS OF COMPARISON ALGORITHMS

No.	Name	Parameter Settings	Literature	Publication Year
1	PIO	Nc1 = 210 (map factor), $Nc2 = 90$ (guideline factor)	[22]	2014
2	OOA	l is between 1 and 2	[23]	2023
3	AO	$\alpha = 0.1, \beta = 0.1, r1 = 1.0$	[24]	2021
4	ННО	E_0 is between 1 and 2, $\beta = 1.5$	[25]	2019
5	COA	l=1.5	[26]	2023
6	GA	pc=0.6,pm=0.3	[16]	1999
7	PSO	$c_1 = 1.2, c_2 = 1.2, w = 0.7$	[17]	1995
8	IVY	β_1 is between 1 and 1.5	[18]	2024
9	IIVY	$k_1 = 1, k_2 = 0.1, \beta = 1.5$	/	/

TABLE II FORMANCE OF COMPARISON ALGORITHMS ON CEC2017

**		D = 50			D = 100				
Name	Mean (B/S/W)	Std (B/S/W)	Best (B/S/W)	Rank	Mean (B/S/W)	Std (B/S/W)	Best (B/S/W)	Rank	
PIO	0/0/1	4/0/6	0/0/0	6	0/2/6	5/3/3	0/0/0	6	
OOA	0/0/6	2/1/1	0/0/0	7	0/0/7	1/7/1	0/0/0	8	
AO	0/1/2	1/0/3	0/0/1	5	1/0/0	2/1/1	0/0/0	5	
ННО	2/1/4	1/3/7	1/0/6	4	1/0/4	1/0/14	1/0/0	4	
COA	0/1/7	1/5/3	0/1/4	7	0/0/7	3/1/3	0/0/1	7	
GA	0/1/7	1/0/1	0/0/0	8	0/0/8	0/0/1	0/0/0	9	
PSO	6/10/4	5/8/3	7/8/6	3	2/14/10	1/2/12	5/5/18	3	
IVY	0/11/10	0/5/4	1/12/11	2	2/12/10	3/0/4	4/16/8	2	
IIVY	21/5/3	14/7/1	20/8/1	1	24/3/2	13/5/0	19/8/2	1	

TABLE III

THE WILCOXON TEST BETWEEN IIVY AND OTHER ALGORITHMS ON CEC2017 BENCHMARK FUNCTIONS (50-D AND 100-D).

	Dimension									
IIVY vs		D =	= 50			D =	= 100			
	p-Value	R^+	R^-	+/=/-	p-Value	R^+	R^-	+/=/-		
PIO	3.61E-04	0.00	435.00	29/0/0	5.75E-06	0.00	435.00	29/0/0		
OOA	4.57E-02	0.00	435.00	29/0/0	1.81E-06	0.00	435.00	29/0/0		
AO	2.60E-05	0.00	435.00	29/0/0	7.16E-06	0.00	435.00	29/0/0		
ННО	2.98E-02	58.00	377.00	28/0/1	8.50E-05	2.00	433.00	28/0/1		
COA	6.40E-04	0.00	435.00	29/0/0	2.29E-05	0.00	435.00	29/0/0		
GA	2.01E-06	0.00	435.00	29/0/0	1.77E-06	0.00	435.00	29/0/0		
PSO	1.45E-01	110.00	335.00	22/0/7	5.82E-02	99.00	336.00	22/0/7		
IVY	1.27E-02	14.00	421.00	28/1/0	3.03E-02	67.00	368.00	25/0/4		
Mean Value	3.34E-02	22.75	412.25	27.9/0.1/1	1.10E-02	21.00	414.00	27.5/0.1/1.5		

 $TABLE\ IV$ Summary of indications mean, STD, best and rank. Results for the classic cec2017 benchmark fuctions (50-d)

r				AO	ННО	COA	GA	PSO	IVY	IIVY
f_1	Mean	5.0467E+07	4.0720E+06	1.3641E+09	1.9665E+05	8.9469E+05	1.0045E+11	4.2407E+10	4.3082E+03	3.8899E+03
	Std	1.3110E+07	2.3629E+06	5.3791E+08	2.6273E+05	1.1299E+06	3.8826E+09	7.1478E+09	6.3049E+03	3.5388E+03
	Best	3.1725E+07	1.5259E+06	5.7839E+08	4.4219E+04	4.0069E+04	9.1459E+10	2.7998E+10	1.0051E+02	5.6110E+02
	Rank	6	5	7	3	4	9	8	2	1
f_3	Mean	1.0903E+05	1.2964E+05	6.7132E+04	3.8944E+04	1.2831E+05	1.9604E+05	1.4848E+05	4.3568E+04	4.4604E+04
	Std	1.3495E+04	1.6664E+04	1.3571E+04	8.9288E+03	1.2966E+04	1.7387E+04	8.2905E+03	1.1641E+04	1.1351E+04
	Best	8.2552E+04	1.0461E+05	3.9045E+04	2.1757E+04	9.6936E+04	1.6306E+05	1.2890E+05	2.5138E+04	2.6585E+04
	Rank	5	7	4	1	6	9	8	2	3
f_5	Mean	8.0126E+02	7.1736E+02	8.0796E+02	7.9673E+02	6.3588E+02	1.1693E+03	1.0697E+03	6.3275E+02	5.5655E+02
, ,	Std	2.7971E+01	3.0554E+01	5.4872E+01	3.1221E+01	2.0849E+01	2.2951E+01	2.1705E+02	5.6397E+01	1.4449E+01
	Best	7.3971E+02	6.4211E+02	7.0205E+02	7.3979E+02	5.7611E+02	1.1064E+03	1.0172E+03	5.9651E+02	5.3283E+02
	Rank	6	4	7	5	3	9	8	2	1
f_7	Mean	1.1945E+03	1.0522E+03	1.1964E+03	1.2991E+03	9.0583E+02	1.9156E+03	1.7023E+03	9.3761E+02	8.0530E+02
Ji	Std	5.6633E+01	5.6900E+01	7.0695E+01	1.3064E+02	3.6210E+01	4.5012E+01	9.4896E+01	6.4798E+01	1.2994E+01
	Best	1.0868E+03	9.8468E+02	1.0877E+03	1.1607E+03	8.4510E+02	1.8338E+03	1.4963E+03	8.4211E+02	7.8365E+02
	Rank	5	4	6	7	2	9	8	3	1
£_	Mean	1.5959E+04	9.5070E+03	1.0826E+04	1.0608E+04	1.9005E+03	3.6806E+04	2.8414E+04	1.3676E+03	9.1268E+02
f_9	Std	1.8104E+03	3.2895E+03	4.0149E+03	2.4563E+03	6.8929E+02	2.0277E+03	2.6945E+03	5.1135E+02	9.1208E+02 1.5790E+01
					6.1102E+03					
	Best Rank	1.1115E+04 7	4.5223E+03 4	5.9037E+03 6	6.1102E+03	1.3813E+03 3	3.1611E+04 9	2.4197E+04 8	9.8130E+02 2	9.0054E+02 1
f			4 2.6645E+04					8 1.8999E+03		
f_{11}	Mean	1.9807E+04		1.1012E+04	5.6072E+03	2.7469E+04	5.0626E+04 1.7894E+04		9.2607E+03	3.6600E+03
	Std	4.6519E+03	2.4977E+03	2.0934E+03	1.2258E+03	1.7478E+03		3.6436E+02	4.5057E+03	7.7584E+02
	Best	1.1548E+04	1.9335E+04	7.1507E+03	3.7623E+03	2.0812E+04	2.5298E+04	1.4436E+03	4.5961E+03	1.7391E+03
c	Rank	6	7	5	3	8 5.2560E-10	9	1 (270)	4	2
f_{13}	Mean	4.9943E+09	5.1097E+10	3.5435E+09	6.4052E+08	5.2569E+10	1.4034E+10	1.6378E+08	7.6530E+08	4.2959E+05
	Std	1.3731E+09	1.4151E+09	1.9964E+09	9.5127E+08	1.4348E+10	1.0525E+10	5.2650E+08	1.2413E+09	1.8906E+05
	Best	1.3173E+09	1.4511E+09	1.9964E+09	3.3169E+07	1.3947E+10	8.8489E+08	3.3452E+04	3.5613E+07	1.9829E+05
	Rank	6	7	8	3	9	5	1	4	2
f_{17}	Mean	6.1213E+03	1.4526E+04	4.1340E+03	3.9491E+03	1.3519E+04	8.1612E+07	8.0310E+03	1.8787E+04	5.4691E+03
	Std	5.5117E+02	1.6664E+04	3.7257E+02	3.9438E+02	1.0235E+04	9.8102E+32	3.4174E+02	7.7956E+02	3.6593E+02
	Best	4.9498E+03	5.2482E+03	3.4684E+03	3.2360E+03	5.2587E+03	4.1205E+34	2.4833E+02	2.7897E+03	2.7816E+03
_	Rank	7	8	5	4	9	6	1	3	2
f_{21}	Mean	3.0026E+03	3.1902E+03	2.8901E+03	2.9969E+03	3.2893E+03	3.4067E+03	2.6793E+03	2.5505E+03	2.4803E+03
	Std	4.3910E+01	9.6283E+01	7.3532E+01	6.5456E+01	8.1169E+01	1.1544E+02	1.0742E+01	7.8800E+01	3.8323E+01
	Best	2.9274E+03	3.0002E+03	2.7177E+03	2.8639E+03	3.1501E+03	3.1964E+03	2.5557E+03	2.4120E+03	2.4238E+03
	Rank	6	7	4	5	8	9	3	1	2
f_{23}	Mean	3.5685E+03	4.5822E+03	3.7600E+03	4.1353E+03	4.5422E+03	4.3169E+03	3.5243E+03	3.0680E+03	2.9386E+03
	Std	5.7172E+01	1.7445E+02	1.8975E+02	2.0459E+02	1.8668E+02	2.7398E+02	1.6463E+02	1.0219E+02	6.5287E+01
	Best		4.1997E+03	3.4361E+03	3.7407E+03	4.2619E+03	3.8184E+03	3.2616E+03	2.8601E+03	2.8205E+03
	Rank	5	8	4	6	9	7	3	2	1
f_{25}	Mean	1.4850E+04	1.5886E+04	6.0873E+04	4.9780E+03	1.5871E+03	2.3342E+04	3.6963E+04	4.1397E+04	3.2217E+03
	Std	1.4353E+03	1.5914E+03	6.4950E+02	5.2466E+02	1.2522E+02	7.0300E+03	3.6108E+03	7.2551E+03	3.6311E+03
	Best	1.1862E+04	1.3021E+04	4.8404E+04	4.0126E+03	1.3457E+04	1.1761E+04	3.1803E+03	3.3330E+03	3.1614E+03
	Rank	7	8	5	4	9	6	2	3	1
f_{27}	Mean	4.3958E+03	8.0670E+03	4.8415E+03	5.5012E+03	6.9768E+03	6.2836E+03	3.8762E+03	4.1006E+03	3.2000E+03
	Std	1.9958E+02	9.5494E+02	3.3459E+02	8.0167E+02	1.0021E+03	6.4330E+02	1.7140E+02	4.4841E+02	1.4392E+02
	Best	3.9412E+03	6.1150E+03	4.1443E+03	4.4232E+03	5.0176E+03	5.2348E+03	3.4328E+03	3.6181E+03	3.2000E+03
	Rank	4	9	5	6	7	8	2	3	1
f_{29}	Mean	8.7530E+03	7.9452E+04	9.1174E+03	8.5613E+03	1.8054E+03	9.9107E+03	5.1992E+03	6.2448E+03	4.6064E+03
	Std	7.8202E+02	8.8033E+04	1.6900E+03	1.7632E+03	2.5486E+03	2.7181E+03	5.4582E+02	2.2384E+03	2.7296E+02
	Best	7.1985E+02	8.2193E+03	6.4534E+02	6.1688E+03	1.8452E+05	7.1146E+03	6.6403E+02	4.7553E+03	3.9563E+03
	Rank	7	8	5	4	9	6	2	3	1
f_{30}	Mean	1.4274E+09	8.1016E+09	3.6485E+08	2.5031E+08	7.6478E+09	1.8561E+08	3.3622E+07	4.1096E+08	5.8912E+07
	Std	4.2075E+09	3.0707E+09	1.7875E+08	1.0194E+07	2.2515E+09	1.6281E+08	1.5654E+07	8.3501E+08	4.5926E+07
	Best	6.7678E+08	1.7077E+09	1.4324E+08	8.9476E+07	3.1963E+09	3.4717E+08	1.5363E+07	1.0833E+07	1.0531E+07
	Rank	7	8	5	4	9	6	3	2	1
Total Rank		179	202	154	124	207	214	105	81	39
Final Rank		6	7	5	4	8	9	3	2	1

 $TABLE\ V$ Summary of indicators mean, STD, Best, and Rank. Results for classic cec2017 benchmark functions (100-d)

f(x)	Index	PIO	OOA	AO	ННО	COA	GA	PSO	IVY	IIVY
f_1	Mean	2.6497E+11	2.7330E+11	1.2987E+11	9.8517E+10	2.7240E+11	5.1887E+10	6.5130E+04	6.6021E+04	4.9345E+04
	Std	1.6886E+10	9.8163E+09	1.1567E+10	1.0147E+10	1.5039E+10	5.6418E+09	1.4889E+04	3.1173E+04	1.0327E+04
	Best	2.2939E+11	2.5310E+11	1.0900E+11	7.4334E+10	2.1405E+11	3.9900E+11	3.8031E+03	3.1764E+04	3.1674E+04
	Rank	7	8	5	4	6	9	3	2	1
f_3	Mean	4.9578E+05	4.5597E+05	2.5760E+05	3.6150E+05	3.5930E+05	9.0638E+04	6.1122E+05	6.8509E+05	3.4288E+05
•	Std	2.1652E+05	1.0797E+05	1.0275E+05	1.5132E04	1.8742E+05	9.9415E+04	9.4176E+05	2.2487E+04	1.4128E+05
	Best	3.6664E+05	3.5163E+05	3.3119E+05	3.0886E+05	3.2319E+05	7.1696E+05	3.8635E+05	3.6407E+05	3.1258E+05
	Rank	7	5	4	1	3	9	8	6	2
f_6	Mean	7.1724E+02	7.1326E+02	6.9411E+02	6.925E+02	7.1225E+02	7.5780E+02	6.7129E+02	6.5732E+02	6.4815E+02
30	Std	3.8910E+00	3.8832E+00	4.9031E+00	3.0546E+00	4.0871E+00	9.5691E+00	5.9275E+00	9.3101E+00	1.1225E+00
	Best	7.0879E+02	7.0284E+02	6.8365E+02	6.8686E+02	7.0012E+02	7.3500E+02	6.5875E+02	6.3279E+02	6.1596E+02
	Rank	7	8	4	5	6	9	3	2	1
f_8	Mean	2.6566E+03	2.9582E+03	2.2288E+03	2.9107E+03	2.6005E+03	3.3665E+03	1.8436E+03	1.8959E+03	1.6833E+03
, 6	Std	6.5244E+01	5.1316E+01	8.2426E+01	3.1551E+01	4.2598E+01	1.9789E+02	8.9003E+01	9.7668E+01	8.7891E+01
	Best	2.5309E+03	2.4812E+03	2.0555E+03	2.0778E+03	2.5128E+03	3.0446E+03	1.6234E+03	1.6723E+03	1.5222E+03
	Rank	8	6	4	5	7	9	2	3	1
f_{10}	Mean	3.3185E+04	3.3652E+04	2.7569E+04	2.5748E+04	3.2525E+04	3.3435E+04	1.9159E+04	1.7721E+04	1.9683E+04
J10	Std	6.1542E+02	7.9490E+02	2.1556E+03	1.1975E+02	9.7051E+02	1.2357E+02	1.5533E+04 1.5533E+02	1.7058E+02	5.5942E+03
				2.1330E+03 2.3839E+04					1.4631E+04	
	Best	3.1809E+04	3.0479E+04		2.3915E+04	2.9478E+04	2.9559E+04	1.6881E+04		1.4550E+04
C	Rank	9 1 0204E - 11	8 2.0048E+11	4 5 0710E - 10	5 2.0(22E+10	6	7 2.7542E+11	3 1 2241E - 10	2	1
f_{12}	Mean	1.0394E+11	2.0948E+11	5.8718E+10	3.9622E+10	2.0560E+11	2.7543E+11	1.2241E+10	1.9062E+10	6.2568E+08
	Std	2.0461E+10	1.5052E+10	1.0345E+09	9.3260E+09	2.1552E+10	5.2277E+10	8.7277E+09	2.3049E+10	1.6038E+08
	Best	6.9962E+11	1.7646E+11	3.5151E+10	2.4961E+10	1.5524E+11	1.7386E+10	2.5566E+10	2.6364E+09	3.3679E+08
_	Rank	6	9	5	4	7	8	2	3	1
f_{14}	Mean	8.8048E+07	9.9349E+07	3.0020E+07	1.3707E+07	8.8570E+07	1.8201E+08	3.5110E+06	1.4215E+07	6.3485E+06
	Std	2.3208E+07	4.0705E+07	9.4977E+06	4.8786E+06	3.6197E+08	1.4135E+08	2.6212E+06	7.1414E+06	2.1418E+06
	Best	4.2960E+07	3.2231E+07	1.2043E+07	5.8057E+06	1.1742E+07	3.7174E+07	6.5856E+05	4.8174E+06	2.2440E+06
	Rank	9	7	6	4	5	8	1	3	2
f_{16}	Mean	1.5046E+04	2.6264E+04	1.3321E+04	1.1550E+04	2.4496E+04	2.4858E+03	7.5315E+03	7.3112E+03	6.2721E+03
	Std	1.0681E+03	3.0251E+03	1.6622E+03	1.5223E+03	3.7997E+03	4.7964E+03	7.9562E+02	8.1185E+02	5.9000E+02
	Best	1.2738E+04	2.0228E+04	1.0276E+03	8.6533E+03	1.8845E+04	1.7772E+03	5.8925E+03	5.4659E+03	5.2082E+03
	Rank	6	9	5	4	8	7	3	2	1
f_{20}	Mean	8.2377E+03	7.6751E+03	6.4688E+03	6.4049E+03	7.7675E+03	8.6745E+03	5.5172E+03	5.8045E+03	5.3456E+03
	Std	3.0318E+02	4.3168E+02	5.9770E+02	5.3071E+02	5.3914E+02	4.9126E+02	6.6819E+02	6.5227E+02	5.3028E+02
	Best	7.4826E+03	6.6732E+03	5.0689E+03	5.0161E+03	6.5262E+03	7.6470E+03	4.0903E+02	4.5775E+03	4.2703E+03
	Rank	8	7	5	4	6	9	1	3	2
f_{22}	Mean	3.5758E+04	3.7423E+04	2.9805E+04	2.8777E+04	3.5059E+04	3.6802E+04	2.1972E+04	2.1632E+04	2.1324E+04
	Std	7.4037E+02	7.9047E+03	1.7049E+03	1.4743E+02	8.3540E+02	1.2981E+03	1.5170E+03	1.0902E+03	4.7400E+03
	Best	3.4411E+04	3.2747E+04	2.5455E+04	2.6587E+04	3.3085E+04	3.3838E+04	1.9028E+04	1.8453E+04	4.0657E+03
	Rank	9	6	4	5	7	8	3	2	1
f_{24}	Mean	6.1947E+03	1.3074E+04	7.1484E+03	8.3454E+03	1.0339E+03	1.2248E+04	6.2070E+03	4.6193E+03	4.3851E+03
	Std	2.5633E+03	7.4782E+02	5.3331E+02	4.7512E+02	6.9710E+02	1.0855E+03	4.0684E+02	3.9142E+02	1.1662E+03
	Best	5.8865E+03	1.1579E+04	6.4486E+03	7.1330E+03	8.9907E+03	1.0436E+04	5.5340E+03	4.1640E+03	3.8680E+03
	Rank	4	9	5	6	7	8	3	2	1
f_{26}	Mean	5.0727E+04	5.3445E+04	3.7013E+04	3.4415E+04	5.3312E+04	6.5220E+04	2.8238E+04	3.0058E+04	1.6509E+04
	Std	9.0344E+03	2.3713E+03	1.9690E+03	2.2797E+03	1.9981E+03	9.0535E+03	2.8621E+03	3.5859E+03	5.8710E+03
	Best	3.0321E+04	4.6845E+04	3.4097E+04	3.0140E+04	4.9606E+04	4.7137E+04	2.2396E+04	2.1881E+04	6.5347E+03
	Rank	5	7	6	4	9	8	3	2	1
f_{28}	Mean	3.3257E+04	3.0249E+04	1.8305E+04	1.3476E+04	3.0695E+04	5.1806E+04	1.1543E+04	9.7394E+03	3.3000E+03
	Std	8.6426E+02	1.1511E+03	1.7212E+03	1.3412E+03	1.3412E+03	7.6391E+03	1.7887E+03	2.3776E+03	1.9574E+04
	Best	3.0715E+04	2.6408E+04	1.5335E+04	2.7073E+04	2.7073E+04	3.5203E+04	8.5376E+03	6.3169E+03	3.3000E+03
	Rank	8	6	5	4	7	9	3	2	1
f_{30}	Mean	9.1010E+09	4.4392E+10	8.7221E+09	3.6434E+09	4.4258E+10	4.5982E+10	7.6979E+08	1.9125E+09	4.4282E+07
7.00	Std	2.6316E+09	5.5663E+09	2.8446E+09	1.6706E+09	7.4825E+09	1.4081E+10	7.4087E+08	1.6865E+09	4.0248E+07
	Best	4.7095E+09	2.8498E+10	2.6907E+09	1.5497E+09	2.5661E+10	2.2207E+10	5.6972E+07	2.6404E+08	9.8039E+06
	Rank	6	9	5	4	8	7	2	3	1
Total Rank		189	217	147	127	209	232	- 77	66	41
Final Rank		6	8	5	4	7	9	3	2	1
Italik					•	,				

 $TABLE\ VI$ Summary of indicators mean, STD, best and rank. Results for classic cec2022 benchmark functions (50-d)

f(x)	Index	PIO	OOA	AO	ННО	COA	GA	PSO	IVY	IIVY
f_1	Mean	9.3759E+10	1.1436E+11	2.1269E+10	5.1947E+09	1.1339E+11	1.1962E+11	7.7279E+09	2.5333E+09	1.0204E+07
	Std	1.5264E+10	7.8285E+09	3.2847E+09	1.5853E+09	9.5890E+09	2.7287E+10	5.4783E+09	4.0990E+09	2.3834E+06
	Best	6.4766E+10	9.6053E+10	1.5848E+10	2.8694E+09	9.3580E+10	7.0049E+10	1.5348E+09	1.1685E+08	6.7925E+06
	Rank	6	9	5	4	8	7	3	2	1
f_4	Mean	4.3747E+06	1.1163E+07	8.5935E+04	1.0880E+04	1.1154E+07	2.9328E+06	9.6396E+03	6.8918E+03	1.9534E+03
	Std	2.3925E+06	4.3153E+06	4.7794E+04	8.1445E+03	3.7820E+06	3.0374E+06	1.3965E+04	1.5106E+04	7.1071E+00
	Best	1.2105E+06	4.5624E+06	2.1255E+04	3.2101E+03	5.0150E+06	1.2838E+05	2.2600E+03	2.0217E+03	1.9375E+03
	Rank	7	8	5	4	9	6	3	2	1
f_6	Mean	2.7867E+03	3.9559E+03	3.7880E+03	5.7485E+03	9.1278E+03	5.1524E+03	5.0545E+03	9.7035E+03	6.9314E+03
	Std	2.4925E+02	4.4559E+02	4.2792E+02	5.2990E+02	1.5852E+03	6.2163E+02	6.4053E+02	1.7355E+03	4.4166E+02
	Best	6.0844E+03	7.3581E+03	3.7409E+03	3.8309E+03	5.9244E+03	4.6010E+03	2.9908E+03	3.2426E+03	2.2455E+03
	Rank	8	9	4	5	6	7	2	3	1
f_8	Mean	1.6528E+04	1.6706E+04	1.3150E+04	1.2059E+04	1.6888E+04	1.7165E+04	1.0053E+04	1.0789E+04	7.9224E+03
	Std	1.8627E+03	4.1661E+02	8.6388E+02	8.9774E+02	5.0251E+02	9.0245E+02	1.1319E+03	9.7155E+02	2.6307E+03
	Best	9.1786E+03	1.5763E+04	1.1202E+04	9.8941E+03	1.6159E+04	1.4439E+04	7.1181E+03	8.4741E+03	2.3174E+03
	Rank	4	7	6	5	9	7	2	3	1
f_{10}	Mean	1.4384E+04	1.6344E+04	4.6934E+03	3.7764E+03	1.5944E+04	1.9612E+04	3.6417E+03	3.4244E+03	3.1459E+03
	Std	6.1542E+02	7.9490E+02	2.1556E+03	1.1975E+02	9.7051E+02	1.2357E+02	1.5533E+02	1.7058E+02	5.5942E+03
	Best	3.1809E+04	3.0479E+04	2.3839E+04	2.3915E+04	2.9478E+04	2.9559E+04	1.6881E+04	1.4631E+04	1.4550E+04
	Rank	9	8	4	5	6	7	3	2	1
Total Rank		34	41	24	23	38	34	13	12	5
Final Rank		7	9	5	4	8	6	3	2	1

 $TABLE\ VII$ SUMMARY OF INDICATORS MEAN, STD, BEST AND RANK. RESULTS FOR CLASSIC CEC2022 BENCHMARK FUNCTIONS (20-D)

f(x)	Index	PIO	OOA	AO	ННО	COA	GA	PSO	IVY	IIVY
f_1	Mean	2.7740E+04	5.4786E+04	6.1955E+04	2.2832E+04	4.1295E+04	8.2669E+04	6.5520E+03	4.8544E+04	2.4780E+04
	Std	7.2716E+03	1.9484E+04	2.6060E+04	8.2846E+03	1.0269E+04	2.2502E+04	5.1785E+03	1.2641E+04	1.0825E+04
	Best	1.7548E+04	2.7120E+04	2.7675E+04	7.8581E+03	2.6306E+04	3.2822E+04	7.8886E+02	2.5085E+04	8.6876E+03
	Rank	3	6	7	9	5	8	1	4	2
f_3	Mean	6.4514E+02	6.7375E+02	6.4251E+02	6.6131E+02	6.7930E+02	7.0246E+02	6.3052E+02	6.0986E+02	6.0024E+02
	Std	7.5110E+00	1.3204E+01	7.6556E+00	9.1668E+00	9.4241E+00	1.4958E+01	1.1484E+01	1.2329E+01	5.1922E-01
	Best	6.3135E+02	6.4159E+02	6.2965E+02	6.3279E+02	6.4956E+02	6.7497E+02	6.1125E+02	6.0001E+02	6.0004E+02
	Rank	5	7	4	6	8	9	3	1	2
f_5	Mean	4.3003E+03	3.3646E+03	2.6171E+03	2.9935E+03	3.4345E+03	1.8577E+03	1.8577E+03	2.3650E+03	2.3724E+03
	Std	9.4769E+02	3.0200E+02	4.1706E+02	3.8044E+02	4.4104E+02	9.4316E+02	6.6412E+02	1.2076E+02	2.0352E+02
	Best	2.4375E+03	2.7269E+03	1.5126E+03	2.1198E+03	2.5750E+03	1.0359E+03	1.0326E+03	2.0420E+03	1.5707E+03
	Rank	7	9	4	6	8	1	2	5	3
f_7	Mean	2.1560E+03	2.1974E+03	2.1285E+03	2.1824E+03	2.1841E+03	2.2547E+03	2.1412E+03	2.1506E+03	2.0676E+03
	Std	2.7634E+01	4.0307E+01	2.3497E+01	4.9523E+01	4.1579E+01	7.3641E+01	5.7697E+01	6.8895E+01	3.3325E+01
	Best	2.1038E+03	2.1283E+03	2.0827E+03	2.1102E+03	2.1094E+034	2.1473E+03	2.0381E+03	2.0682E+03	2.0292E+03
	Rank	5	8	4	7	6	9	2	3	1
f_9	Mean	2.5996E+03	3.6238E+03	2.5983E+03	2.5481E+03	3.2815E+03	2.7231E+03	2.4943E+03	2.4868E+03	2.4759E+03
	Std	3.8975E+01	3.8476E+02	4.4460E+01	4.6707E+01	2.6089E+02	1.0039E+02	1.9968E+01	4.1605E+00	1.9669E+00
	Best	2.5419E+03	3.0380E+03	2.5198E+03	2.4927E+03	2.8073E+03	2.5952E+03	2.4808E+03	2.4809E+03	2.4731E+03
	Rank	6	9	5	4	8	7	2	3	1
Total Rank		26	39	24	32	35	34	10	16	9
Final Rank		5	9	4	6	7	8	2	3	1

 $TABLE\ VIII$ THE WILCOXON TEST BETWEEN IIVY AND OTHER ALGORITHMS ON CEC2020 AND CEC2022 BENCHMARK FUNCTIONS (20-D AND 50-D)

	Dimension									
IIVY vs		CEC	72020			CEC	72022			
	p-Value	R^+	R^-	+/=/-	p-Value	R^+	R^-	+/=/-		
PIO	3.62E-11	0.00	55.00	10/0/0	6.03E-02	22.00	56.00	7/0/5		
OOA	3.02E-11	0.00	55.00	10/0/0	8.97E-04	1.00	77.00	11/0/1		
AO	1.34E-09	0.00	55.00	10/0/0	4.68E-02	9.00	69.00	9/0/3		
ННО	1.36E-07	0.00	55.00	10/0/0	8.73E-02	3.00	75.00	10/0/2		
COA	3.05E-11	0.00	55.00	10/0/0	3.90E-03	1.00	77.00	11/0/1		
GA	3.02E-11	0.00	55.00	10/0/0	6.12E-04	1.00	77.00	11/0/1		
PSO	8.30E-02	14.00	41.00	7/0/3	1.36E-01	16.00	62.00	8/0/4		
IVY	7.61E-05	2.00	53.00	9/0/1	7.57E-02	3.00	75.00	10/0/2		
Mean Value	1.19E-02	2.00	53.00	9.5/0/0.5	5.15E-02	7.00	71.00	9.6/0/2.4		

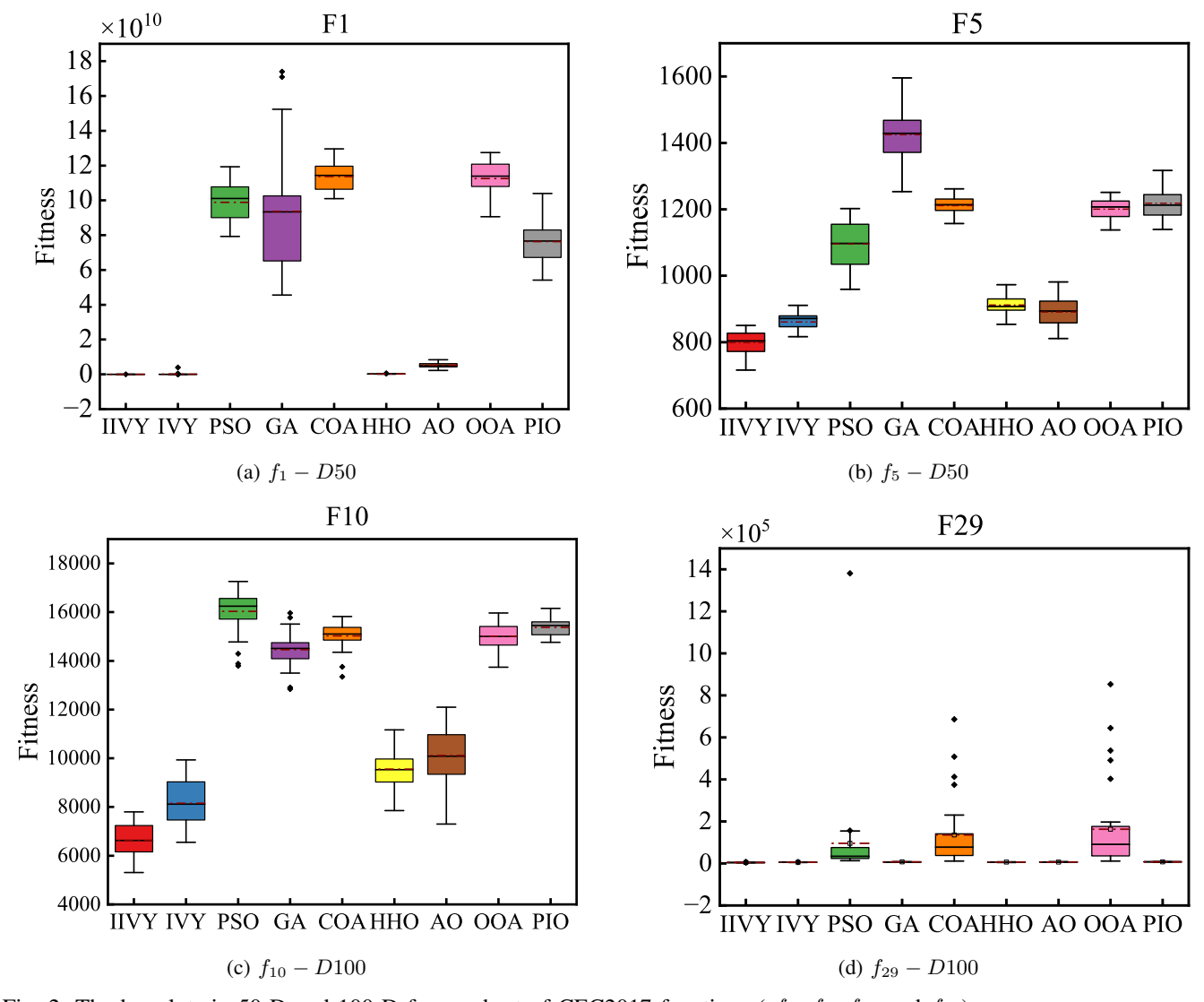


Fig. 2: The boxplots in 50-D and 100-D for a subset of CEC2017 functions (f_1 , f_5 , f_{10} and f_{29}).

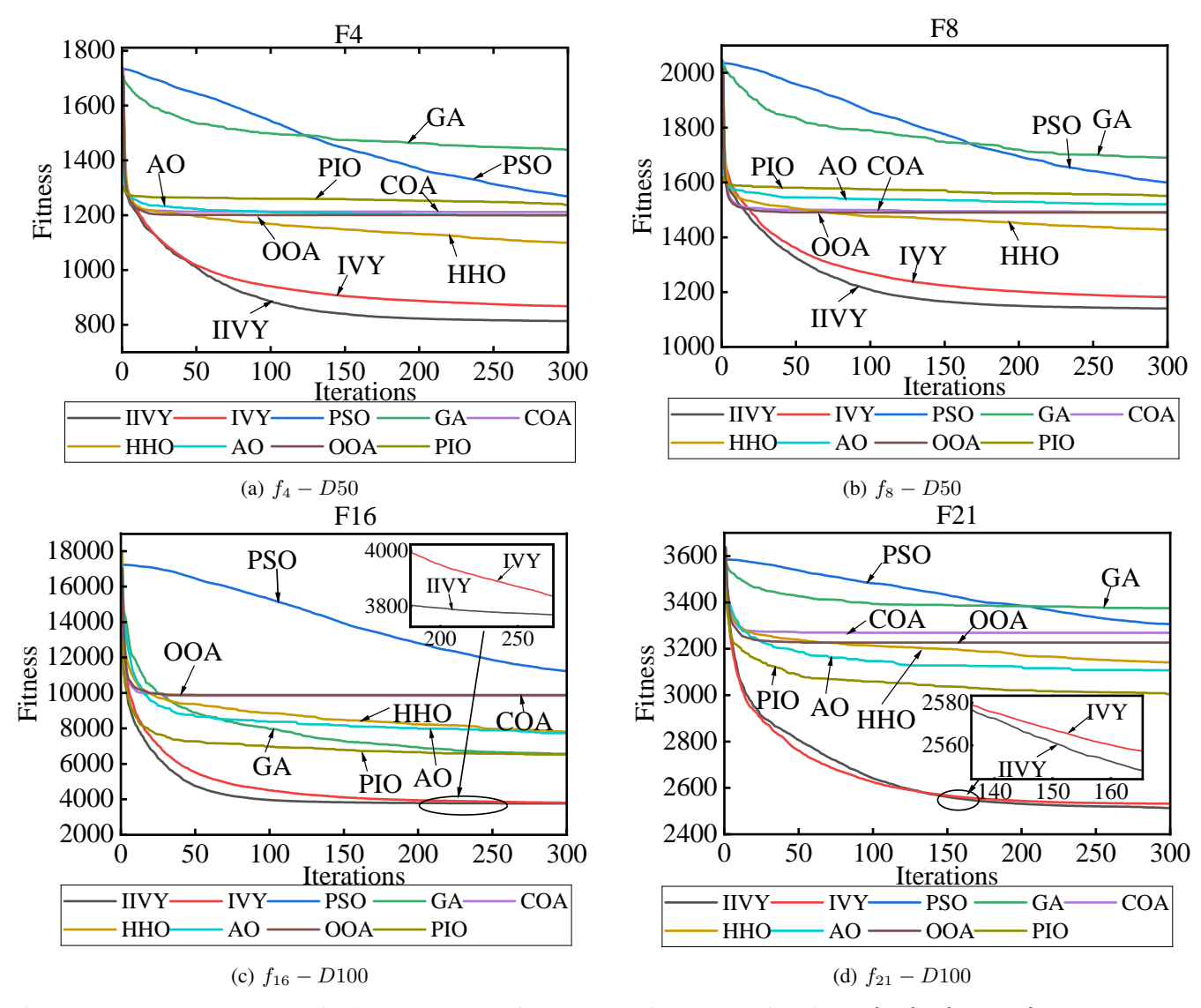


Fig. 3: The convergence curves in 50-D and 100-D for a subset of CEC2017 functions (f_4 , f_8 , f_{16} and f_{21}).

Statistical analysis results (see Table III and Table VIII) on widely used and authoritative benchmark suites CEC2017, CEC2020, and CEC2022 further strongly confirm the overall and consistent performance advantage of the IIVY algorithm. In Table III (CEC2017, D = 50 vs. D = 100), the detailed and comprehensive comparisons of IIVY with PIO [22], OOA [23], AO [24], HHO [25], COA [26], GA [16], PSO [17], and the basic IVY [18] very clearly show that most obtained p-values from Wilcoxon's rank-sum test are far well below the strict 0.05 threshold, strongly indicating that the performance differences are indeed highly statistically significant for the great majority of considered test functions. At the same time, the observed R^+ values for several compared algorithms are very close to zero, while the corresponding R^- values approach the maximum possible level, meaning that IIVY consistently and reliably outperforms on almost all tested functions and therefore exhibits a clear, strong, and convincing competitive edge. This demonstrated superiority steadily holds consistently in both medium (D = 50) and high (D = 100) dimensions, thereby convincingly demonstrating excellent robustness across different dimensional scales.

In Table VIII (CEC2020 vs. CEC2022), the dominance of

IIVY remains evident. The p-values for most comparisons again fall below 0.05 on both test suites, while the R^+ and R^- distributions are heavily skewed in favor of IIVY. For example, in the CEC2022 benchmarks, R^+ values for IIVY against some algorithms remain in the low single digits, whereas the corresponding R^- values exceed 70, highlighting its adaptability and strong global search capability on more challenging problems.

Taken together, the results in Table III and Table VIII indicate that IIVY maintains consistent advantages across different dimensions and demonstrates strong generalization across benchmark sets and problem categories. These findings show that IIVY achieves high accuracy and efficiency on diverse, complex optimization tasks and holds promising potential for practical applications.

V. APPLICATION OF MPPT FOR PHOTOVOLTAIC SYSTEMS

A. Solar Model Building

In PV power generation systems, PV modules serve as the core component, converting sunlight directly into electrical energy through the photovoltaic effect. The conversion process is highly sensitive to environmental conditions, particularly solar irradiance and temperature. Irradiance mainly determines the PV current magnitude, while temperature primarily influences parameters such as open-circuit voltage [9]. Accurate estimation of PV array output current, voltage, and power therefore requires explicit consideration of these two variables [14].

To evaluate the combined effects of irradiance and temperature on PV output—and to address the dynamic optimization requirements of MPPT algorithms [27]—this work employs the single-diode equivalent circuit model. The model incorporates series resistance (R_s) and shunt resistance (R_{sh}) to capture ohmic losses, enabling a realistic representation of module behavior. This approach allows dynamic performance analysis and provides closed-form expressions for key variables. MPPT plays a critical role by continuously adjusting the operating point of the PV system to achieve maximum available power under changing conditions [28].

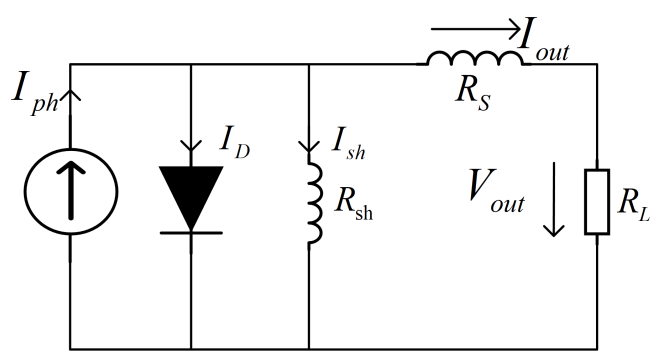


Fig. 4: Equivalent circuit of the solar cell diode model.

In Fig. 4, I_{ph} denotes the photo-generated current, I_D is the diode current, and I_{sh} is the current through R_{sh} . R_s represents the series resistance, R_L the load resistance, and U and I are the terminal voltage and current. From Fig. 4, the PV cell output current I_{out} is given as:

$$I_{out} = I_{ph} - I_D - I_{sh} \tag{15}$$

where I_{ph} is the photocurrent, I_D the diode current, and I_{sh} the shunt branch current. As described in [14], I_{ph} can be expressed as a function of irradiance G and temperature T:

$$I_{ph} = \frac{G}{G_0} \cdot [I_{ph0} + \mu_{sc} \cdot (T - T_0)] \tag{16}$$

where G is irradiance, T is ambient temperature, and μ_{sc} is the short-circuit current temperature coefficient. I_{ph0} and T_0 denote the standard test condition values, with T_0 typically $25^{\circ}\mathrm{C}$.

The diode current is defined as:

$$I_D = I_0 \cdot \exp\left(\frac{V_{out} + I_{out} \cdot R_s}{a}\right) - 1 \tag{17}$$

where I_0 is the diode reverse saturation current, V_{out} is the terminal voltage, R_s is the series resistance, and a is the thermal voltage factor:

$$a = \frac{N_s \cdot A \cdot k \cdot T}{q} \tag{18}$$

with A the diode ideality factor, N_s the number of series-connected cells, k the Boltzmann constant $(1.381 \times 10^{-23} \text{ J/K})$, and q the electron charge $(1.602 \times 10^{-19} \text{ C})$.

The parallel current I_p is described as [27]:

$$I_{p} = \frac{V_{out} + R_{s} \cdot I_{out}}{R_{p}}$$

$$I_{0} = \left[I_{SC_{0}} \cdot \exp\left(-\frac{V_{OC}}{a}\right)\right] \cdot \left(\frac{T}{T_{0}}\right)^{3} \cdot \exp\left[\left(\frac{qE_{g}}{Ak}\right) \cdot \left(\frac{1}{T_{0}} - \frac{1}{T}\right)\right]$$
(20)

where I_{SC_0} is the short-circuit current, V_{OC} the open-circuit voltage, and E_q the bandgap energy of the material.

As noted in [10], the current-voltage (I-V) characteristics can be obtained by sweeping voltage values to compute the current response. The power-voltage (P-V) curve is then derived from $P=V\cdot I$ [29]. Figure 5 illustrates the I-V characteristics of the PV module, with the MPP marked, showing how MPPT varies with irradiance and temperature.

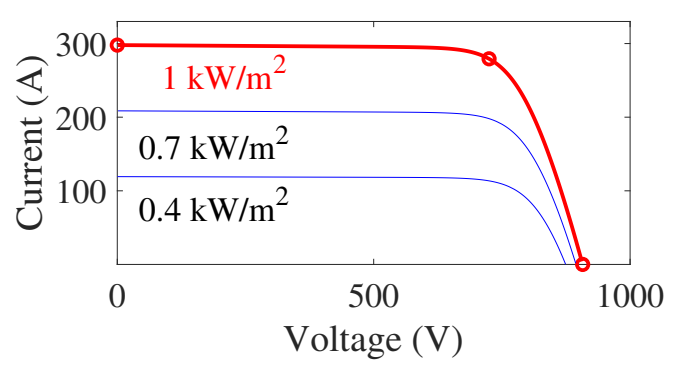


Fig. 5: I-U characteristic curve of PV cell with constant T and varying S

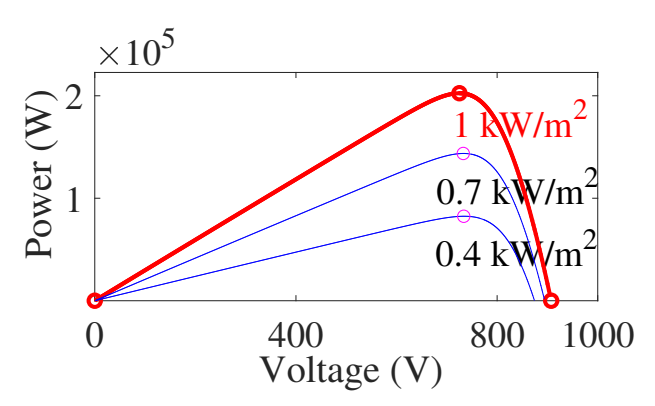


Fig. 6: P-U characteristic curve of PV cell with constant T and varying S

The P-V curve is further analyzed in Fig. 6. The results highlight that MPPT is strongly influenced by fluctuating irradiance, typically caused by unpredictable weather. This variability creates a dynamic optimization challenge requiring continuous MPPT adaptation. The simulation conditions used for Figs. 5 and 6 are: temperature 25°C and irradiance values of 1000 W/m², 700 W/m², and 400 W/m². These results clearly demonstrate that environmental changes directly affect maximum power output, emphasizing the need for robust MPPT algorithms.

B. Maximum Power Point Tracking

Assuming the MPP varies with temperature and irradiance, dynamic optimization is necessary. As noted in [29],

DC/DC converters adjust impedance to regulate power, with control parameters depending on topology. Duty cycle and conversion ratio are discussed in [30], while [31] relates these to equivalent resistance and PV terminal voltage. MPPT controllers are essential under dynamic conditions [32]. The P&O method adjusts duty cycle to reach the maximum power point, combining simplicity with low cost. The improved IVY-based MPPT algorithm offers better efficiency, MPP localization, and faster response under irradiance changes, reducing stabilization time.

C. MPPT Application Based on IIVY

To evaluate the effectiveness of MPPT algorithms, a case study was implemented in MATLAB/Simulink, with the system topology shown in Fig. 7.

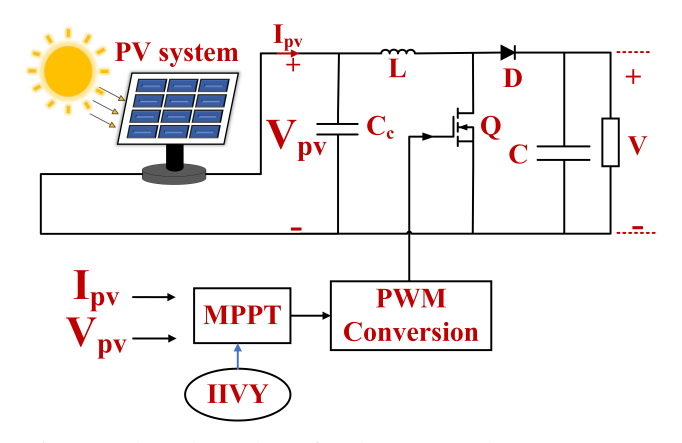


Fig. 7: Selected topology for the case study.

PV arrays: To capture a broad, diverse, and comprehensive range of realistic photovoltaic operating scenarios, the irradiance conditions were systematically, carefully, and consistently varied during the controlled experimentation process. Three representative, practically meaningful, and frequently encountered levels were specifically selected: high (1000 W/m², clear sky conditions), medium (700 W/m², moderately cloudy conditions), and low (400 W/m², heavily overcast weather). These deliberately chosen and well-defined conditions therefore provide reliable, realistic, and convincing coverage of PV system operation under diverse, typical, and naturally occurring real-world weather patterns.

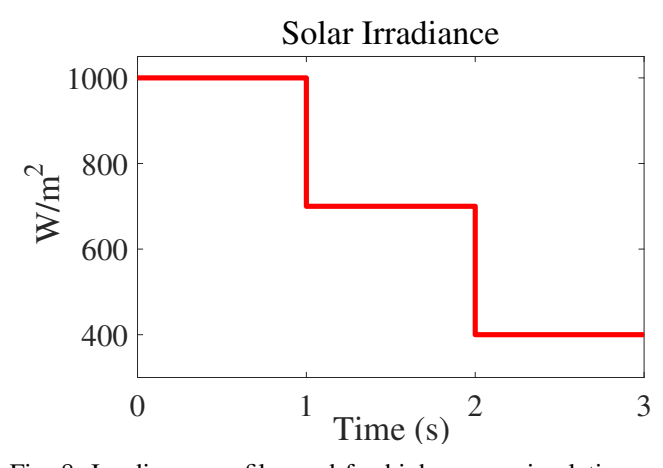


Fig. 8: Irradiance profile used for high power simulations

Besides irradiance and temperature. the configuration of the PV array also strongly and directly influences the overall dynamic system behavior. Important parameters such as the number of series/parallel interconnected modules, the module power ratings, and the intrinsic electrical properties together determine the actual output power, operational efficiency, stability, and transient dynamic response. To ensure higher accuracy and reliability, this study explicitly specifies the detailed PV array characteristics, including precise electrical ratings (e.g., V_{OC} , I_{SC}), design specifications, and interconnection structure information.

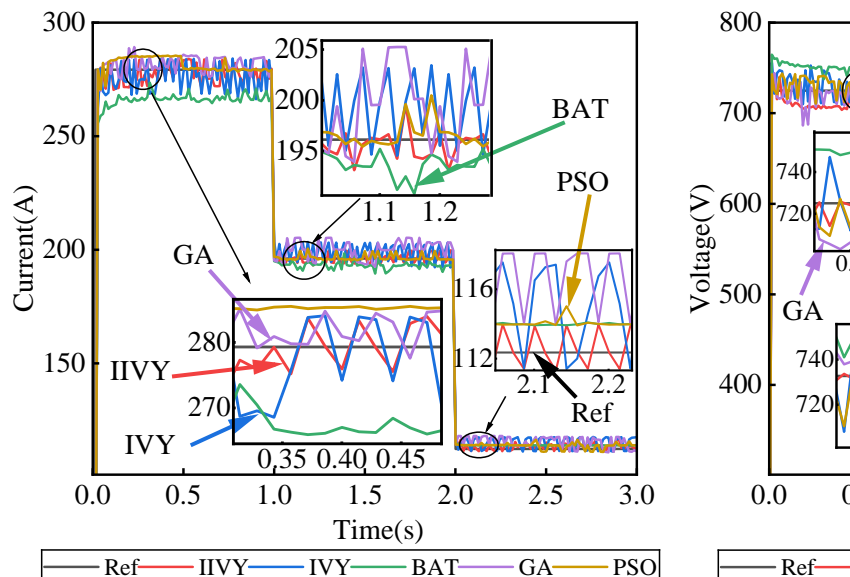
TABLE IX
CONVERTER PARAMETERS

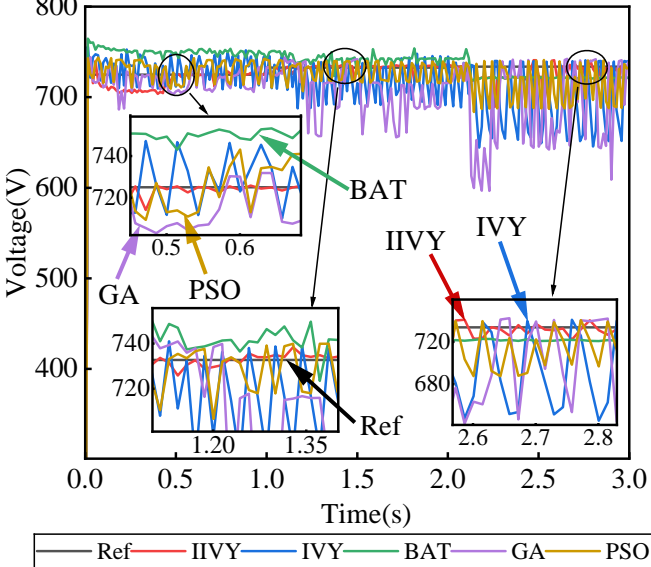
Parameter	Value
Input voltage	725 V
Switching frequency	10 kHz
Duty cycle	3.5%
Inductance	$3~\mu\mathrm{H}$
Capacitance	$408~\mu\mathrm{F}$
Load resistance	$2.69~\Omega$
Output power	209.48 kW
Output voltage	750 V
Output current	279.3 A

TABLE X
PV ARRAY SIMULATION PARAMETERS

Parameter	Value
Maximum power	213.15 W
Cells per module	60
V_{OC}	36.3 V
I_{SC}	7.84 A
V_{MPP}	29 V
I_{MPP}	7.35 A
Temp. coefficient of V_{OC}	-0.33%/°C
Temp. coefficient of I_{SC}	0.102%/°C
I_L	7.8495 A
I_O	9.9124E-11 A
Diode ideality factor	0.9386
R_{sh}	340.283 Ω
R_s	$0.41237~\Omega$
Parallel strings	38
Series strings	25

Results: The improved IIVY algorithm was thoroughly benchmarked against four widely used and well-established MPPT methods under the MATLAB/Simulink simulation environment. The diverse test cases deliberately included abrupt irradiance variations and sudden load perturbations, thereby allowing a more systematic and comprehensive evaluation of transient response, steady-state tracking precision, overall accuracy, and robustness against multiple external disturbances. The corresponding detailed results and performance comparisons are clearly shown in Figs. 9 and 10.





(a) Current harvested over time under different irradiance conditions. (b) Voltage harvested over time under different irradiance conditions.

Fig. 9: Voltage, and current harvested over time under different irradiance conditions.

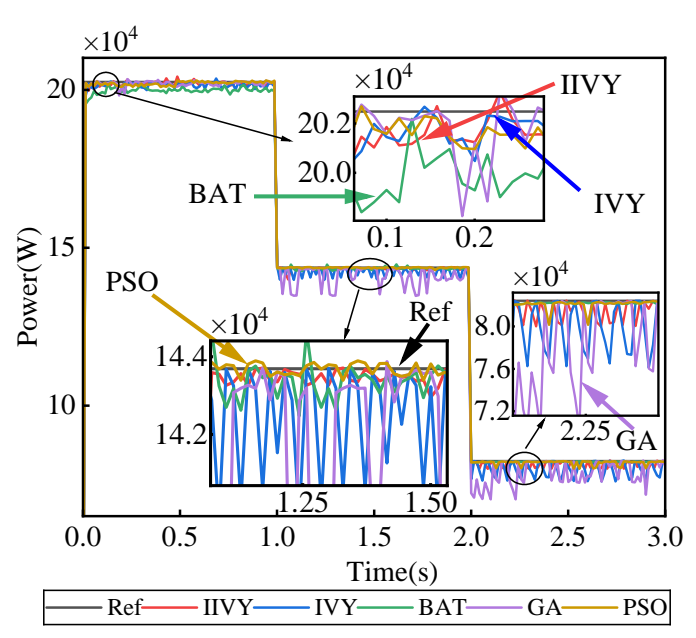


Fig. 10: Power harvested over time under different irradiance conditions.

The IIVY algorithm was tested at irradiance levels of 1000, 700, and 400 W/m², with ambient temperature fixed at 25°C. Results indicate rapid convergence, with the maximum power point reliably tracked within 0.15–0.25 s, significantly improving response speed. During sudden irradiance changes, IIVY adapts quickly, showing lower overshoot and reduced oscillations compared to other methods. Current ripple was also notably suppressed, minimizing power loss and component stress. Power stability improved markedly: fluctuations decreased by approximately 17% at 1000 W/m², by 20% at 400 W/m², and by up to 78% under highly variable conditions. These results confirm the adaptability and robustness of IIVY under diverse operating scenarios.

VI. CONCLUSION

In this paper, an improved IIVY algorithm is proposed to address the problems of the traditional IVY algorithm, such as the lack of initial population diversity, weak local search ability, and fixed convergence step. It consists of three strategies: optimizing the initial population generation through inverse learning to improve the population diversity and global search ability; introducing the Lévy flight update strategy to enhance the ability of the algorithm to jump out of the local optimum and maintain the search equilibrium; and adopting the adaptive convergence factor and dynamically adjusting the step size to balance the global exploration and the local exploitation, so as to improve the convergence speed and the solution accuracy.

First, the experimental results (Table IV and Table V) on 30 low- and high-dimensional benchmark functions show that IIVY significantly outperforms eight representative optimization algorithms, including PIO, OOA, AO, COA, HHO, and the original IVY, in all dimensions and problem types. In the low-dimensional case, IIVY ranks first on 20 functions and second on 8 functions; in the high-dimensional case, it ranks first on 19 functions and second on 8 functions. Visualization comparisons (Fig. 2 and Fig. 3) further validate its advantages in convergence speed, global search capability, and jumping out of local optima. The statistical test results (Table III) also prove that IIVY significantly outperforms the comparison algorithms at the significance level of 0.05 and obtains the best average ranking in Friedman's test, highlighting its robustness and wide applicability. Secondly, in PV MPPT applications, IIVY demonstrates fast convergence (0.15-0.25 s), low tracking error, low current fluctuation, and 17%-78% reduction in output power fluctuation under different irradiance $(1000/700/400 \text{ W/m}^2)$ and 25°C conditions. 78% of the output power fluctuation. The experimental results show that the algorithm is able to lock the maximum power point stably and efficiently when the irradiance changes rapidly, with excellent dynamic response and robustness, which significantly improves the energy capture efficiency and operational stability of the photovoltaic system.

Future research can further explore the extended application of IIVY in practical engineering scenarios such as multi-objective optimization, hybrid energy storage scheduling, microgrid control, etc., in order to give full play to its optimization potential.

REFERENCES

- [1] M. Rehan and M. M. A. Awan, "Optimization of MPPT Perturb and Observe Algorithm for a Standalone Solar PV System," *Mehran University Research Journal of Engineering & Technology*, vol. 43, no. 3, pp. 136–149, 2024.
- [2] T. Liu, H. Yu, S. Liu, J. Tong, Z. Wu, and Q. Yuan, "Photovoltaic MPPT Tracking Under Partial Shading Based on ICS-IGSS-INC Hybrid Algorithm." *Engineering Letters*, vol. 33, no. 2, pp. 215–222, 2025.
- [3] S. Tabassum, T. Rahman, A. U. Islam, S. Rahman, D. R. Dipta, S. Roy, N. Mohammad, N. Nawar, and E. Hossain, "Solar Energy in the United States: Development, Challenges and Future Prospects," *Energies*, vol. 14, no. 23, p. 8142, 2021.
- [4] N. Kalaiarasi, A. Sivapriya, P. Vishnuram, M. Pushkarna, M. Bajaj, H. Kotb, and S. Alphonse, "Performance Evaluation of Various Z-Source Inverter Topologies for PV Applications Using AI-Based MPPT Techniques," *International Transactions on Electrical Energy* Systems, vol. 2023, no. 1, p. 1134633, 2023.
- [5] G. Singh Chawda, O. Prakash Mahela, N. Gupta, M. Khosravy, and T. Senjyu, "Incremental Conductance Based Particle Swarm Optimization Algorithm for Global Maximum Power Tracking of Solar-PV Under Nonuniform Operating Conditions," *Applied Sciences*, vol. 10, no. 13, p. 4575, 2020.
- [6] L. Li, G. Zeng, and B. Wen, "Enhanced Maximum Power Point Tracking Capability of Grid-connected Solar PV Based on Improved Bacterial Foraging Optimization." *Engineering Letters*, vol. 33, no. 6, pp. 1896–1902, 2025.
- [7] J. C. Ugaz Peña, C. L. Medina Rodríguez, and G. O. Guarniz Avalos, "Study of a New Wave Energy Converter with Perturb and Observe Maximum Power Point Tracking Method," *Sustainability*, vol. 15, no. 13, p. 10447, 2023.
- [8] J. Xue and B. Shen, "A Novel Swarm Intelligence Optimization Approach: Sparrow Search Algorithm," Systems Science & Control Engineering, vol. 8, no. 1, pp. 22–34, 2020.
- [9] S. Allahabadi, H. Iman-Eini, and S. Farhangi, "Fast Artificial Neural Network Based Method for Estimation of the Global Maximum Power Point in Photovoltaic Systems," *IEEE Transactions on Industrial Electronics*, vol. 69, no. 6, pp. 5879–5888, 2021.
- [10] T. Liu, S. Liu, H. Yu, B. Ma, J. Tong, Z. Wu, and Q. Yuan, "Hybrid Optimization for Photovoltaic Power Systems: Enhancing MPPT with Improved Whale and Particle Swarm Algorithms." *Engineering Letters*, vol. 33, no. 6, pp. 1746–1758, 2025.
- [11] R. A. Marques Lameirinhas, J. P. N. Torres, and J. P. de Melo Cunha, "A Photovoltaic Technology Review: History, Fundamentals and Applications," *Energies*, vol. 15, no. 5, p. 1823, 2022.
- [12] D. Maradin, "Advantages and Disadvantages of Renewable Energy Sources Utilization," *International Journal of Energy Economics and Policy*, vol. 11, no. 3, pp. 176–183, 2021.
- [13] S. R. D. Naoussi, K. T. Saatong, R. J. J. Molu, W. F. Mbasso, M. Bajaj, M. Louzazni, M. Berhanu, and S. Kamel, "RETRACTED ARTICLE: Enhancing MPPT Performance for Partially Shaded Photovoltaic Arrays through Backstepping Control with Genetic Algorithm-optimized Gains," *Scientific Reports*, vol. 14, no. 1, p. 3334, 2024.
- [14] Z. M. S. Elbarbary and M. A. Alranini, "Review of Maximum Power Point Tracking Algorithms of PV System," Frontiers in Engineering and Built Environment, vol. 1, no. 1, pp. 68–80, 2021.
- [15] M. Kermadi, Z. Salam, A. M. Eltamaly, J. Ahmed, S. Mekhilef, C. Larbes, and E. M. Berkouk, "Recent Developments of MPPT Techniques for PV Systems Under Partial Shading Conditions: A Critical Review and Performance Evaluation," *IET Renewable Power Generation*, vol. 14, no. 17, pp. 3401–3417, 2020.

- [16] J. Shapiro, "Genetic Algorithms in Machine Learning," in Advanced Course on Artificial Intelligence. Springer, 1999, pp. 146–168.
- [17] J. Kennedy and R. Eberhart, "Particle Swarm Optimization," in *Proceedings of ICNN'95-international Conference on Neural Networks*, vol. 4. ieee, 1995, pp. 1942–1948.
- [18] M. Ghasemi, M. Zare, P. Trojovský, R. V. Rao, E. Trojovská, and V. Kandasamy, "Optimization Based on the Smart Behavior of Plants with Its Engineering Applications: Ivy Algorithm," *Knowledge-Based Systems*, vol. 295, no. 1, p. 111850, 2024.
- [19] A. W. Mohamed, A. A. Hadi, A. M. Fattouh, and K. M. Jambi, "LSHADE with Semi-parameter Adaptation Hybrid with CMA-ES for Solving CEC 2017 Benchmark Problems," in 2017 IEEE Congress on Evolutionary Computation (CEC). IEEE, 2017, pp. 145–152.
- [20] C.-T. Yue, K. V. Price, P. N. Suganthan, J.-J. Liang, M. Z. Ali, B.-Y. Qu, N. H. Awad, and P. Biswas, "Problem Definitions and Evaluation Criteria for the CEC 2020 Special Session and Competition on Single Objective Bound Constrained Numerical Optimization," *Computational Intelligence Laboratory Technical Report*, vol. 201911, no. 11, pp. 1–24, 2020.
- [21] A. Kumar, K. V. Price, A. W. Mohamed, A. A. Hadi, and P. N. Suganthan, "Problem Definitions and Evaluation Criteria for the CEC 2022 Special Session and Competition on Single Objective Bound Constrained Numerical Optimization," Nanyang Technological University Technical Report, vol. 202211, no. 11, pp. 1–20, 2021.
- [22] H. Duan and P. Qiao, "Pigeon-inspired Optimization: A New Swarm Intelligence Optimizer for Air Robot Path Planning," *International Journal of Intelligent Computing and Cybernetics*, vol. 7, no. 1, pp. 24–37, 2014.
- [23] M. Dehghani and P. Trojovský, "Osprey Optimization Algorithm: A New Bio-inspired Metaheuristic Algorithm for Solving Engineering Optimization Problems," Frontiers in Mechanical Engineering, vol. 8, p. 1126450, 2023.
- [24] L. Abualigah, D. Yousri, M. Abd Elaziz, A. A. Ewees, M. A. Al-Qaness, and A. H. Gandomi, "Aquila Optimizer: A Novel Meta-heuristic Optimization Algorithm," *Computers & Industrial Engineering*, vol. 157, no. 11, p. 107250, 2021.
- [25] A. A. Heidari, S. Mirjalili, H. Faris, I. Aljarah, M. Mafarja, and H. Chen, "Harris Hawks Optimization: Algorithm and Applications," *Future Generation Computer Systems*, vol. 97, no. 8, pp. 849–872, 2019.
- [26] M. Dehghani, Z. Montazeri, E. Trojovská, and P. Trojovský, "Coati Optimization Algorithm: A New Bio-inspired Metaheuristic Algorithm for Solving Optimization Problems," *Knowledge-Based Systems*, vol. 259, p. 110011, 2023.
- [27] B. Yang, T. Zhu, J. Wang, H. Shu, T. Yu, X. Zhang, W. Yao, and L. Sun, "Comprehensive Overview of Maximum Power Point Tracking Algorithms of PV Systems Under Partial Shading Condition," *Journal* of Cleaner Production, vol. 268, no. 15, p. 121983, 2020.
- [28] Y. Deng, X. Zhang, G. Zhang, and X. Han, "Adaptive Neural Tracking Control of Strict-feedback Nonlinear Systems with Event-triggered State Measurement," ISA Transactions, vol. 117, no. 11, pp. 28–39, 2021.
- [29] A. Refaat, Q. A. Ali, M. M. Elsakka, Y. Elhenawy, T. Majozi, N. V. Korovkin, and M. H. Elfar, "Extraction of Maximum Power from PV System Based on Horse Herd Optimization MPPT Technique Under Various Weather Conditions," *Renewable Energy*, vol. 220, no. 1, p. 119718, 2024.
- [30] H. M. Ashraf, M. Elahi, and C.-H. Kim, "A Novel Technique Using Stretching, Repulsion, and Chimp Optimization Algorithm to Find Global Maximum Power Point Considering Complex Partial Shading Conditions," *International Journal of Circuit Theory and Applications*, vol. 52, no. 3, pp. 1322–1341, 2024.
- [31] S. Ngo, C.-S. Chiu, and T.-D. Ngo, "A Novel Horse Racing Algorithm Based MPPT Control for Standalone PV Power Systems," *Energies*, vol. 15, no. 20, p. 7498, 2022.
- [32] C. Mai, L. Zhang, X. Chao, X. Hu, X. Wei, and J. Li, "A Novel MPPT Technology Based on Dung Beetle Optimization Algorithm for PV Systems Under Complex Partial Shade Conditions," *Scientific Reports*, vol. 14, no. 1, p. 6471, 2024.



Yuhang Kang is a postgraduate student at the School of Electronic and Information Engineering, University of Science and Technology Liaoning, Anshan China. Her research interests include renewable energy power generation and nonlinear control systems.



Lei Liu was born in Liaoning, China, in 1981. She received her Master's degree in Geotechnical Engineering from the University of Science and Technology Liaoning in 2010. She is currently an associate professor at the Yingkou Institute of Technology. Her research interests include renewable energy power generation and energy storage.



Lidong Wang (Corresponding Author) was born in Liaoning province, China in 1971, received the B.S. and M.S. degrees from Harbin Institute of Technology and University of Science and Technology Liaoning, China in 1993 and 2004 respectively, and he received Ph.D. degree from Gyeongsang National University, Korea in 2008. His research interests include nonlinear system control, pattern recognition, machine learning and digital signal processing.



control systems.

Zhongfeng Li (Corresponding Author) was born in Liaoning, China, in 1981, received the M.S. degrees from University of Science and Technology Liaoning in 2008. He is currently a Ph.D. candidate at the School of Electronic and Information Engineering, University of Science and Technology Liaoning, Anshan, China, and an associate professor at the School of Electrical Engineering, Yingkou Institute of Technology, Yingkou, China. His research interests include renewable energy power generation and nonlinear



Mingyang Liu is a postgraduate student at the School of Electronic and Information Engineering, University of Science and Technology Liaoning, Anshan China. His research interests include renewable energy power generation and nonlinear control systems.



Zhenlong Zhao was born in Liaoning, China, in 1982, received the M.S. degrees from University of Science and Technology Liaoning in 2009. He is an associate professor at the School of Electrical Engineering, Yingkou Institute of Technology, Yingkou, China. His research interests include industrial robot system.